Analytica Chimica Acta 1227 (2022) 340323

Contents lists available at ScienceDirect

Analytica Chimica Acta

journal homepage: www.elsevier.com/locate/aca

CHA-based dual signal amplification immunofluorescence biosensor for ultrasensitive detection of dimethomorph

Yunyun Wang, Haonan Ruan, Jing Zhang, Yudan Wang, Mengyue Guo, Tongwei Ke, Jiaoyang Luo **, Meihua Yang *

Key Laboratory of Bioactive Substances and Resources Utilization of Chinese Herbal Medicine, Ministry of Education, Institute of Medicinal Plant Development Chinese Academy of Medical Sciences & Peking Union Medical College, Beijing, 100193, China

HIGHLIGHTS

- A single-strand DNA and DMM antibody co-modified AuNP probe was constructed.
- A dual signal amplification platform was accomplished by combining nanomaterials technology and CHA strategy.
- Ultrasensitive fluorescent detection limit of DMM was estimated to be as low as 0.002 ng/mL.
- The developed IMF biosensor achieved good specificity and excellent detection capabilities in multiple complex substrates.

GRAPHICAL ABSTRACT

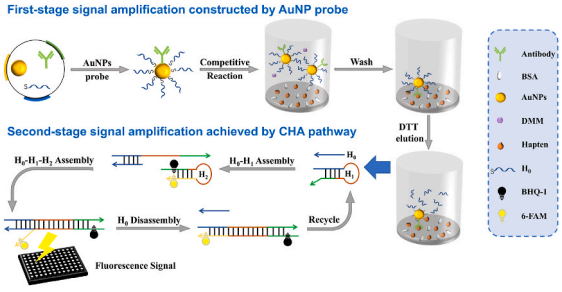

ARTICLE INFO

Keywords:
Immunofluorescence biosensor
Dual signal amplification
Dimethomorph detection
AuNP probe
Catalytic hairpin assembly

ABSTRACT

Dimethomorph (DMM) is a widely used high-efficiency fungicide which poses unpredictable threats to the ecological environment and public health. It is significant to establish a sensitive and robust analytical method for DMM detection. Here, we fabricated a catalytic hairpin assembly (CHA) - based immunofluorescence (IMF) biosensor by using single-strand DNA and DMM antibody co-modified gold nanoparticles (H_0-Ab-Au) as anti-interference probes and DMM antigen coated 96-well plate as the immune recognition element and CHA reaction vessel. Parameters relevant to AuNP probes preparation and CHA reaction environment were optimized. After optimization, the LOD of 0.002 ng/mL was calculated, with a linear correlation in inverse proportion to DMM concentration ranging from 0.01 ng/mL to 50 ng/mL. In addition, the developed biosensor was successfully applied to a variety of complex matrix samples, with satisfactory recoveries over a range of 86.74%–118.60%. Moreover, the detection results of IMF biosensor have a good correlation with liquid chromatography-tandem mass spectrometry (LC-MS/MS). Therefore, our proposed IMF biosensor exhibits ultra-high sensitivity and excellent specificity, as well as great potential for application to other hazards.

* Corresponding author.
** Corresponding author.
E-mail addresses: jyluo@implad.ac.cn (J. Luo), mhyang@implad.ac.cn (M. Yang).

https://doi.org/10.1016/j.aca.2022.340323
Received 19 July 2022; Received in revised form 23 August 2022; Accepted 23 August 2022
Available online 27 August 2022

1. Introduction

Dimethomorph (DMM), a broad-spectrum and highly efficient fungicide belonging to morpholine chemical family, is used to control late blight and downy mildew. Despite its beneficial agricultural effects, DMM is frequently detected in agricultural products, medicinal herbs, soil and groundwater [1–3] and has also been detected in human hair [4]. These levels of contamination could pose risks to human health and environmental safety, particularly through soil and water pollution [5,6], hormonal system intervention [7] and neurotoxic effects [8,9]. Therefore, many nations or regions have set strict standards regarding the maximum residue limit (MRL) of DMM, including China [10], European Union [11], the United States [12], Japan [13] and Korea [14]. For example, the limit of DMM for medicinal herbs set by GB 2763–2021 was 0.1–20 mg/kg, while the European Union suggested a limit of 0.01 mg/kg for most vegetables. To meet these strict standards, it is important to quickly and accurately detect DMM in diverse matrices, necessitating the development of a facile and reliable analytical method.

Traditional chromatography methods for DMM detection require expensive instruments and complex sample pretreatment, making them time-consuming and labor-intensive [1,15]. The existing electrochemical and immunochromatographic methods are susceptible to laboratory environmental conditions, resulting in unstable output signals or low sensitivity [7,16,17]. The fluorescence detection method has high sensitivity [18], but the narrow detection range limits its application. With rapid development in nanomaterials technology and fluorescent signal amplification strategies, catalytic hairpin assembly (CHA) is an enzyme free signal amplification technology enabled by an approach of toehold-mediated strand displacement, which has the superiority of mild reaction condition and easy programmable strand design, possessing significant capacity in the enhancement of small molecule detection sensitivity [19]. Over the years, CHA-based biosensors emerged with the combination of a variety of analytical techniques including surface enhanced Raman scattering [20], colorimetry [21] and electrochemistry [22]. Remarkably, the fluorescence method is convenient, fast and highly sensitive in practical applications [23–25]. Furthermore, gold nanoparticles (AuNPs) are facile to prepare and exhibit good biocompatibility, making them splendid substrates for novel biosensor fabrication [26].

In the present work, an immunofluorescence (IMF) biosensor for high throughput and high sensitivity detection of DMM was developed by combining AuNP functional nanomaterial with CHA signal amplification strategy. As illustrated in Scheme 1, gold nanoparticles are co-modified with DMM antibodies and oligonucleotide trigger chains (H_0) as the CHA reaction probes, and the large surface area of AuNPs allows the loading of more H_0 chains to realize first stage signal amplification. The target DMM are pre-formulated in different concentrations. Subsequently, the AuNP probes and target DMM undergo an immune-competitive reaction with DMM antigen coated in 96-well plate. The competitive binding of DMM to the antibody on the surface of AuNP probes prevents the AuNP probes from binding to the antigen on the microplate. After the competitive reaction, unbound AuNP probes and target DMM are washed away, and then dithiothreitol (DTT) can be used to elute trigger chain H_0 from AuNPs bound in the plate. The CHA reaction is initiated as H_0 chains are released into the solution. H_0 chains can induce the opening of H_1 hairpins, thus exposing the binding sequence to hybridize with H_2 hairpins, the opened H_1 chain assembles with H_2 hairpin to form an H_1–H_2 dimer, releasing H_0 chain for the next cycle. With the progression of the CHA reaction, quenched 6-FAM fluorescence is released from opened H_2 hairpins to realize second stage signal amplification, and the observed fluorescence intensity was in inverse proportion to DMM concentration. In the absence of H_0 chain, the recurring CHA reaction does not occur, resulting in low background signal.

2. Materials and methods

2.1. Materials and reagents

DMM and other fungicides (metalaxyl, metalaxyl-M, benalaxyl, flutolanil and carbendazim) standard solution (100 μg/mL, dissolved in methanol) was purchased from Alta scientific (Tianjin, China). Deionized water used in this study was purified by Milli-Q system. The DMM antigen and monoclonal antibody (mAb) from mouse ascites were provided by Beijing Kwinbon Biotechnology Co. Ltd. (Beijing, China). Dithiothreitol (DTT), 4 S Red Plus solution and bovine serum albumin (BSA) and was purchased from Sangon Biotech (Shanghai) Co., Ltd. HAuCl4 and K_2CO_3 was obtained from Macklin (Shanghai, China). Black 96-well plates were purchased from Corning, Inc. (Corning, NY, USA). Polyethylene glycol (PEG) 20000 was obtained from Beijing Solarbio Science & Technology Co., Ltd. (Beijing, China). *P. notoginseng* and *P. ginseng* were collected from Yunnan province in China, and cucumber and grape samples were purchased from a local supermarket in Beijing.

All buffers were prepared with double-distilled water as follows: 0.01 M phosphate buffered saline (PBS, pH 7.4); salting buffer (0.01 M PBS, 2.0 M NaCl); washing buffer (PBST) (0.01 M PBS, 0.05% Tween-20); blocking and storage buffer (0.01 M PBS, 1% PEG 20000, 1% BSA).

2.2. Synthesis of AuNP probes

All glassware used in this study for the preparation of AuNPs solution were immersed for 12 h with aqua regia acid solution (HCl: HNO_3, 3:1)

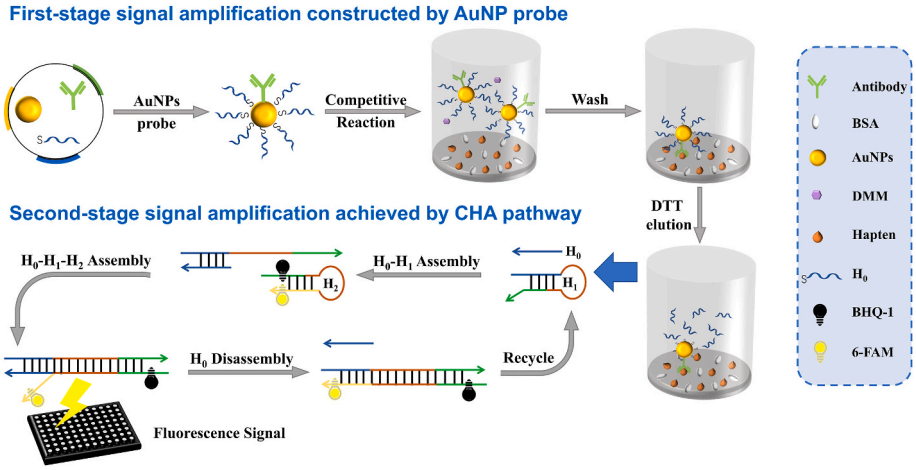

Scheme 1. Illustration of the immunofluorescence biosensor for DMM detection based on dual signal amplification.

and completely cleaned with ultrapure water. A fresh stock of 13 nm gold colloidal solution was synthesized through the trisodium citrate reduction method [27]. Briefly, 50 mL hydrogen tetrachloroaurate (III) trihydrate solution (1 mM) was prepared in a three necked bottle and heated to a vigorous boil under magnetic stirring. Immediately, 5 mL sodium citrate tribasic solution (38.8 mM) was added. As the reaction progressed, the color of the mixed solution turned from yellow to colorless, then to black-purple and finally wine red. Heating continued for 15 min until the reaction was complete. And then the solution was cooled down at room temperature and filtered through a 0.22 μm cellulose nitrate membrane filter. The prepared AuNPs solution was stored at 4 °C and characterized using transmission electron microscopy (TEM, JEM-1200EX, Japan JEOL) and UV–Vis spectroscopy (G9821A, Agilent Technologies Inc, American). The preparation of AuNP probes were achieved by the modification of DMM antibodies and oligonucleotide trigger chains (H_0) [28]. First, 0.1 M K_2CO_3 was used to adjust 1.0 mL AuNPs solution to pH 8.5–9.0, after which different volumes of DMM antibody (0.5 mg/mL) were mixed to form Ab-Au complexes and incubated at room temperature for 1 h. The minimum additive amount of DMM antibody was determined via flocculation test, a certain amount of antibodies modified on the surface of AuNPs can resist the aggregation caused by sodium chloride [29]. After optimizing DMM antibody concentration, 0.2 OD (optical density) thiolated H_0 was introduced and immobilized on the surface of AuNPs as H_0-Ab-Au probes via –SH bonds. Afterwards, the final concentration of 1% PEG 20000 and 0.15 M salting buffer was added respectively, after which the solution was incubated for 2 h at 4 °C. Subsequently, 1% BSA was added to reduce non-specific reactions on the AuNPs surface and incubated for another 1 h at 37 °C. Then, the H_0-Ab-Au probes solution was centrifugated at 13000 rpm for 15min, and washed twice with PBS buffer for the purpose of remove excess unbound antibody and oligonucleotides. Finally, blocking and storage buffer was used to redispersed the prepared probes and stored at 4 °C for use in subsequent experiments.

2.3. Preparation of hairpin chain

The designed sequences with reference to relevant literature [30] are listed in Table S1. All DNA oligonucleotides used in the preparation of probes and CHA reaction were synthesized and purified by Shanghai Bio-Engineering Company (Shanghai, China). Thiolated H_0 was dissolved in Tris-HCl buffer (10 mM Tris-HCl, 1 mM ethylenediaminetetraacetic acid, pH 8.5) at a concentration of 50 μM, which was used to immobilized on the surface of AuNPs. Two hairpin substrate chains (H_1 and H_2) were mixed in the Tris-HCl/Na^+/Mg^{2+} buffer (40 mM Tris-HCl, 8 mM $MgCl_2$, 100 mM NaCl, pH 8.5) at concentration of 50 μM. While H_2 chain folded into hairpin structure, the FAM fluorescence was quenched by proximal BHQ at the end of the toe strand. Before use, H_1 and H_2 were heated for 5 min at 95 °C, then incubated for 1 h at 37 °C to guarantee the stable and complete formation of hairpin structures. As shown in Table S2, four reaction systems of H_0, H_1 and H_2 were prepared to verify the feasibility of the designed CHA pathway. The total volume of each well was supplemented to 130 μL with PBS buffer, and the samples were reacted for 80 min at 37 °C before fluorescence and electrophoresis analysis.

2.4. 20% polyacrylamide gel electrophoresis analysis

Gel contents (as list in Table S3) were mixed and casted into a gel assembly unit immediately after addition of the catalyst, then polymerized at room temperature for about 30 min. The prepared gel was pre-run for 10min at 300 V in 0.5 × TBE to streamline the gel pores. Then, 10 μL of each sample solution mixed with 2 × loading buffer were loaded separately into each channel and subjected to electrophoresis in 0.5 × TBE at 200 V for 90 min. A control sample containing ladder (20 bp) was also run in parallel with the experimental samples. After being stained for 20 min by diluted 4 S Red Plus solution, the gel was visualized using Image Lab™ Touch software (Bio-Rad, America).

2.5. Fluorescence detection of DMM

For the detection of DMM, 100 μL DMM antigen solution was first incubated for 3 h at 37 °C in a black polystyrene microplate. After washing four times with PBST, 100 μL 1% BSA was used to block the bare surface of microplate and incubated at 37 °C for 1 h to reduce non-specific immune responses. Subsequently, 50 μL real sample extract spiked different concentrations of DMM standard was mixed with 50 μL PBS buffer (0.01 M, pH 7.4) diluted AuNP probes and incubated at 37 °C for 30 min. After the immune competitive reaction between DMM antibody modified AuNP probes with DMM molecules and DMM antigens coated on the microplate, unbound fungicides and AuNP probes were washed four times by PBST. Lastly, 100 μL DTT solution (10 mM, 0.6 M NaCl) was added to displace the trigger chain H_0 by ligand exchange [28], after which samples were mixed with H_1 (10 μL, 0.5 μM) and H_2 (10 μL, 0.5 μM) at 37 °C for 80 min. After the CHA reaction, fluorescence measurements were obtained using a spectrofluorophotometer (Tecan infinite M1000 Pro, Männedorf, Switzerland) with the excitation wavelength set as 485 nm, and emission wavelengths from 500 nm to 600 nm were recorded.

2.6. Real sample application

The effectiveness of developed IMF biosensor was investigated on real samples, *P. notoginseng*, *P. ginseng*, cucumber and grape were pretreated and spiked with different concentration of DMM fungicide according to previously described methods [31]. All samples were confirmed by LC-MS/MS to be free from DMM fungicides. First, a certain amount of real sample was extracted with 10 mL of methanol/water (60:40, v/v) by ultrasonicating for 10 min. The sample amount of *P. notoginseng* and *P. ginseng* powder was 1.0 g; while the water content of fresh cucumber and grape samples is larger, it was set to 5.0 g to avoid uneven sampling. For IMF biosensor assays, samples were centrifuged for 5 min at 6000 rpm, after which the supernatant was filtered through a 0.22 μm nylon membrane and diluted with PBS for analysis. For LC-MS/MS detection [32], 1.0 g NaCl and 4.0 g anhydrous $MgSO_4$ were added to samples after ultrasonication. The mixture was shaken for 5 min immediately, then centrifuged for 5 min at 6000 rpm. Next, transferred 2 mL of supernatant to a 10 mL centrifuge tube containing 100 mg C18 and 100 mg PSA. The tubes were shaken for 5 min and centrifuged at 6000 rpm for another 5 min. Finally, the supernatant was passed through a 0.22 μm cellulose nitrate membrane filter before proceeding with LC-MS/MS (See supplement materials).

3. Results and discussion

3.1. Characterization of AuNPs and H_0-Ab-Au probes

AuNPs were synthesized by trisodium citrate reduction method, which is pioneered by Turkevich [33] and further refined by Frens [27]. It is clearly seen from Fig. S1 that the gold nanoparticles were obtained in consistent diameter size of 13 nm with good dispersion, and a maximum UV absorbance peak was observed at 520 nm. For the flocculation test shown in Fig. 1, aggregation can be observed as a red-to-blue color change (Fig. 1a), and the redshift of ultraviolet absorbance at λ_{max} was also measured (Fig. 1b and c). From these data, 4 μg/mL was selected as the appropriate amount for Ab-Au complex formation.

Subsequently, thiolated H_0 trigger chains were added to the Ab-Au complex solution to synthesis H_0-Ab-Au probes via –SH bonds. A 1–2 day step-wise salt aging process was often used on the attachment of negatively charged DNA strands to gold nanoparticles [34]. To avoid the time-consuming salting process, we introduced a surfactant to stabilize this conjugate suspension. Sodium dodecyl silicate (SDS, 1%) and

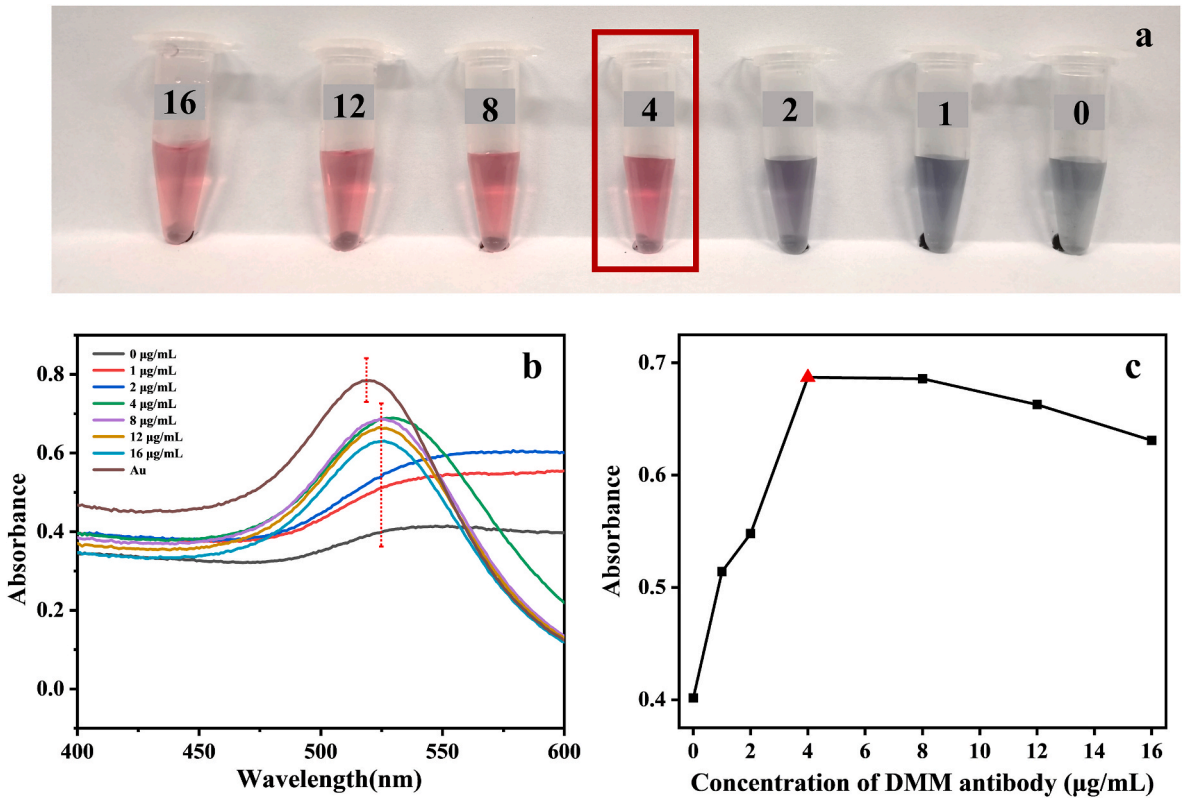

Fig. 1. Optimization of DMM antibody addition amount by flocculation test. (a and b) The color change and UV–vis spectrum of the AuNPs solution added different antibody amount (μg/mL); (c) absorbance of antibody concentrations at 0–16 μg/mL. (For interpretation of the references to color in this figure legend, the reader is referred to the Web version of this article.)

polyethylene glycol (PEG 20000, 1%) were compared for use in the preparation of AuNP probes. It was demonstrated in Fig. 2a that the color of the dispersion system prepared using SDS was lighter, while the fluorescence intensity of the PEG dispersion system was twice higher than that of SDS; therefore, PEG 20000 was selected as the dispersant for probe preparation. Bovine serum albumin (BSA, 1%) was also added to mask remaining free sites on the AuNPs and prevent further nonspecific binding. The successful formation of H_0-Ab-Au probes were confirmed by monitoring the maximum ultraviolet absorbance peak in the wavelength range of 400–800 nm, which exhibited a red-shift from 518 to 526 nm. In addition, the color of functionalized AuNPs became deeper as shown in Fig. 2b. According to the TEM images shown in Fig. 2c and d, shadows were also visible surrounding modified AuNPs, while absent from bare AuNPs, indicating successful preparation of H_0-Ab-Au probes.

3.2. Feasibility of CHA strategy

Herein, the feasibility of CHA reaction was first proved by 20% native polyacrylamide gel electrophoresis analysis. As shown in Fig. 3a, the bands in lane 1 and 2 represent H_1 and H_2, respectively. The cross-interaction between H_1 and H_2 was effectively blocked in the absence of H_0 (lane 3), indicating that H_1 and H_2 can stably coexist in solution as hairpins structure. Upon the addition of H_0 (lane 4), a new band appeared, corresponding to a stable H_1–H_2 duplex and demonstrating that H_0 initiate the hybridization of H_1 and H_2. The assemblies of the designed hairpins were further characterized by fluorescence measurement, as shown in Fig. 3b. The mixed solution of H_1 and H_2 exhibited weak fluorescence emission at 520 nm, mainly because the FAM fluorescent group in the folded H_2 hairpin structure was effectively quenched by the adjacent BHQ group. However, after H_0 was added, the mixed solution exhibited an obviously enhanced fluorescence signal, indicating that H_0 initiates the assembly process to open the folded H_2 hairpin structure, separating the FAM group from the BHQ group. The result was consistent with that of the PAGE assay, further confirming the feasibility of the CHA reaction.

3.3. Optimization of experimental parameters

In order to maximize the analytical performance of this IMF biosensor, we optimized the pH value used in the probe preparation process and several parameters related to the CHA reaction system, including the concentrations of DTT (Dithiothreitol) and NaCl, and the ratio of H_1 to H_2. pH value can affect the rate of coupling between the antibody and DNA strands on gold nanoparticles. It has been reported that maximal adsorption of proteins occurs at a pH close to or slightly above that protein's isoelectric point (pI), and pH 8.0–9.0 is the optimal for antibody coupling [29]. A novel method for the attachment of DNA strands to AuNPs surface in a few minutes using pH 3.0 citrate buffer has also been reported [35]. Under general consideration, we investigated the effects on the probe preparation process of AuNP solution alone (pH 7.8) and AuNP solutions containing a gradient of 0.2 M K_2CO_3 with increasing pH values. The results, as shown in Fig. 4, indicated that fluorescence intensity was the highest using AuNPs solution alone, which was selected for further optimization.

The synthesized H_1 and H_2 hairpin chains are important components of this biosensor that, emit detectable fluorescence signals through the CHA reaction. Research on fluorescence signal amplification strategies has attracted wide interest in recent years. Some studies have directly modified DNA strand-labeled fluorophores onto gold nanoparticles, potentially damaging the fluorophore during the probe preparation process and, resulting in low fluorescence efficiency [36,37]. In the present study, independently isolated hairpin strands H_1 and H_2 were synthesized, and added prior to the CHA reaction, reducing the loss of fluorescence and maximizing fluorescence efficiency. What is

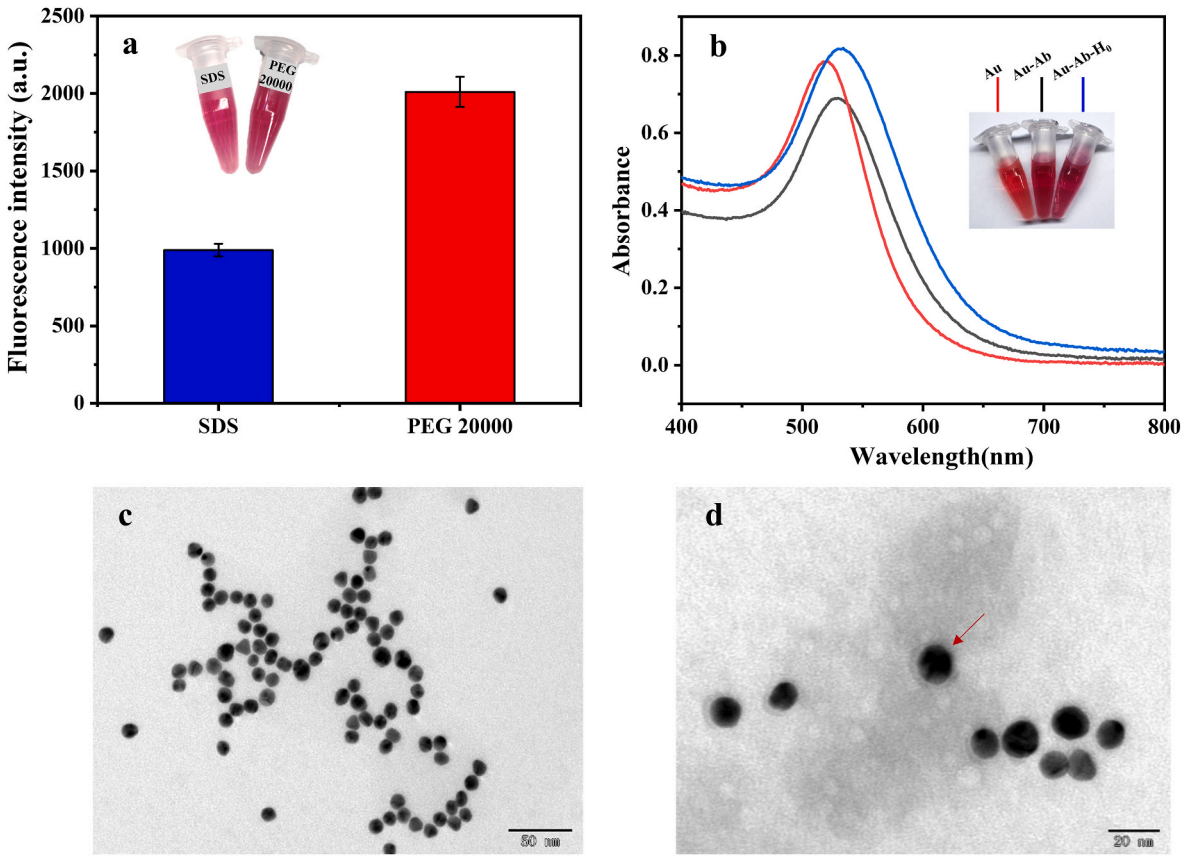

Fig. 2. Characterization of gold nanoparticles and H_0-Ab-Au probes. (a) Comparison the fluorescence effect of two surfactants in the preparation of probes; (b) UV/Vis spectrum of unmodified gold nanoparticles and the modification of DMM antibody and CHA trigger chain; (c and d) TEM image of unmodified gold nanoparticles and H_0-Ab-Au probes. (For interpretation of the references to color in this figure legend, the reader is referred to the Web version of this article.)

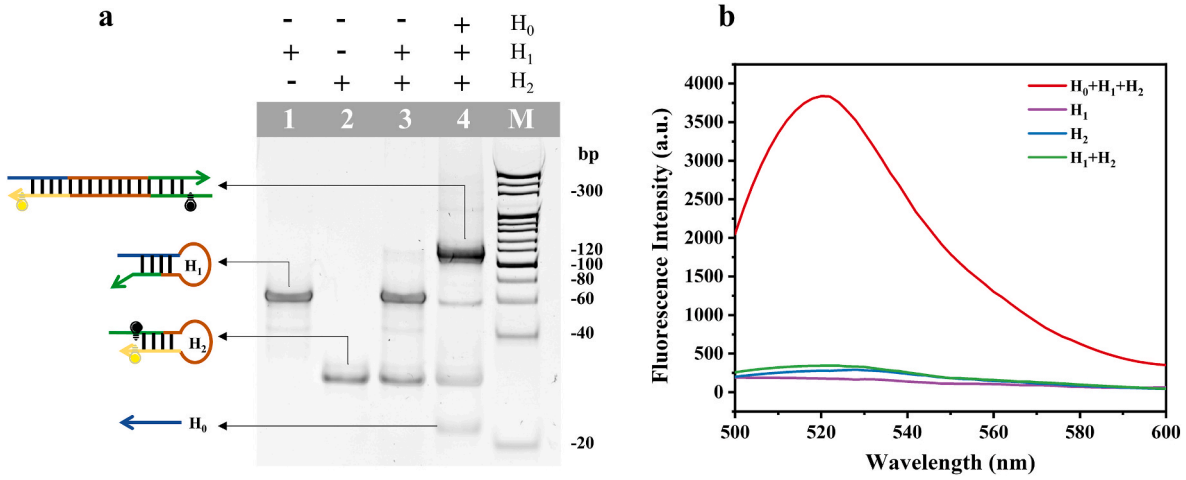

Fig. 3. Feasibility of CHA strategy in 20% native PAGE (a) and fluorescence measurement (b); Lane 1: H_1, Lane 2: H_2, Lane 3: H_1+H_2, Lane 4: H_0+H_1+H_2.

noteworthy is that the ratio of H_1 to H_2 significantly affects the fluorescent signal amplification efficiency. Low concentrations of H_1 and H_2 output weak signals, which can affect the sensitivity of fluorescence detection, thus sufficient H_1 and H_2 amounts are required to complete enough rounds of CHA cycles. However, excess may also spontaneously initiate hybridization between H_1 and H_2, causing the release of high background fluorescence from the opened H_2 hairpin structure. As Fig. 4b shown, the fluorescence intensity was enhanced by the increasing proportions of H_1 until a ratio of 2:1 was reached. Hence, an optimum ratio of 2:1 was selected for the CHA reaction.

The IMF biosensor developed herein relies on a disulfide reducing agent, dithiothreitol (DTT) [38], to implement ligand-exchange process in order to elute covalently adsorbed thiolated oligonucleotides (H_0) from the AuNPs surface for fluorescence readout. Moreover, the ligand exchange method enhances the assay's high sensitivity and maintains its reliability, both simplifying the assay operation and boosting its quantitative capabilities. In addition, the appropriate increasement of salt concentration used in the DTT elution buffer may enhance scanometric results, which is depending on oligonucleotide sequence [28]. For these reasons, the concentrations of DTT and NaCl were optimized. As shown

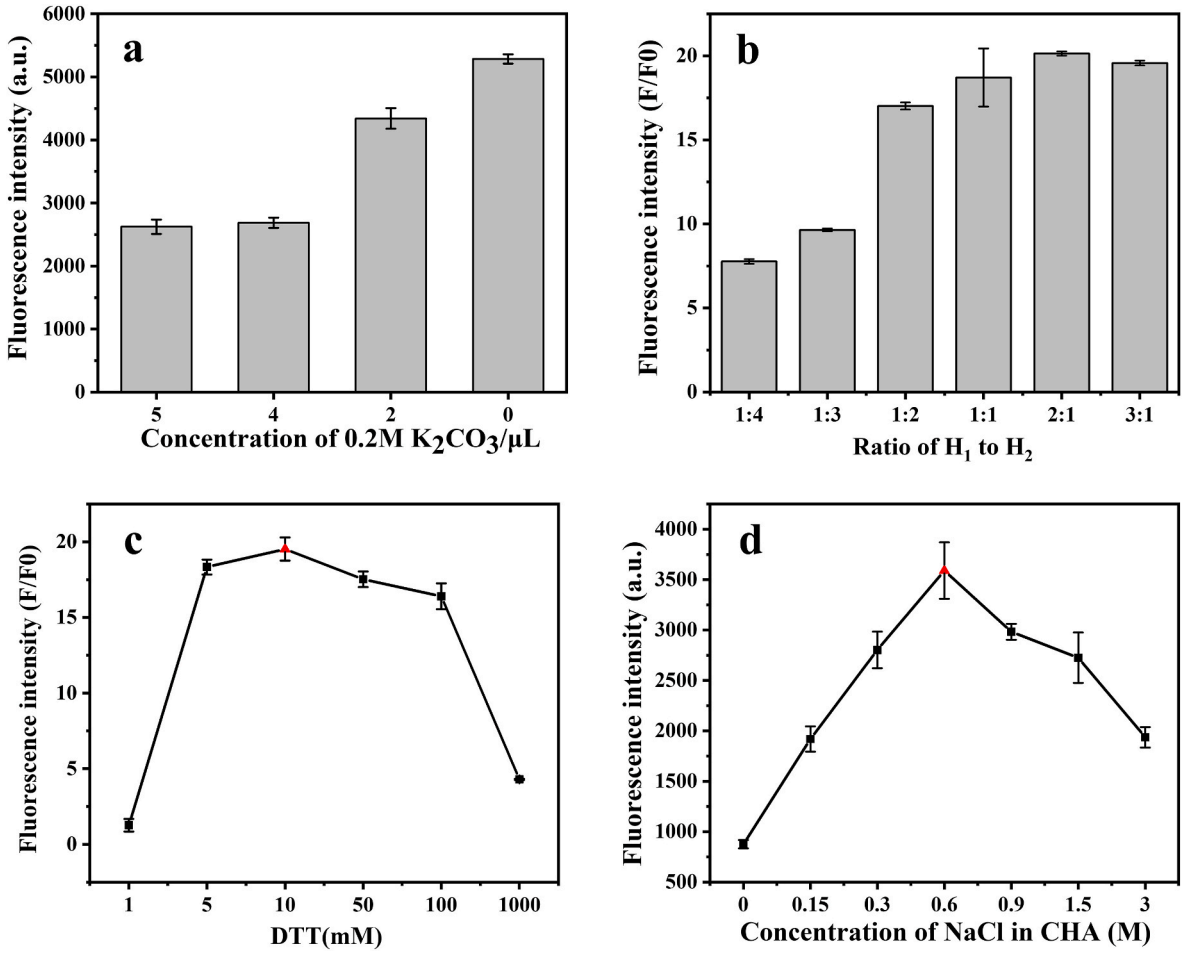

Fig. 4. Optimization of the experimental parameters. (a) pH value in the probe preparation process; (b) ratio of H_1 to H_2; (c) concentration of DTT; (d) concentration of NaCl. The fluorescence intensity was employed to establish the optimal experimental conditions, F/F0 represents the fluorescence intensity of the catalyzed reaction in test samples relative to the uncatalyzed background in blank samples. Error bars represent the standard deviations of three experiments.

in Fig. 4c and d, CHA catalytic efficiency was clearly enhanced in assay buffer containing 10 mM DTT and 0.6 M NaCl.

3.4. Analytical performance and selectivity of IMF biosensor

Under optimized conditions, the sensing capability of this DMM fungicide detection biosensor was investigated to construct a standard curve. According to Fig. 5a, increasing concentrations of DMM molecules were associated with a concentration dependent decrease in fluorescence. The fluorescence intensity exhibits a good linear relationship with the logarithm of DMM concentrations in the range of 0.01–50 ng/mL ($R^2 = 0.99274$) is shown in Fig. 5b. The limit of detection (LOD) for DMM was found to be 0.002 ng/mL, calculated as the average fluorescence intensity for seven blank samples plus three times of the standard deviation [39], 20–5000 times higher than those of existing reported DMM detection methods. As summarized in Table 1, currently reported sensing systems for DMM detection include electrochemical, fluorometric, spectrophotometric and immunochromatographic methods. Our proposed IMF biosensor exhibits a relatively wide linear detection range and exerts an obvious increase in sensitivity due to the application of a dual signal amplification strategy. Furthermore, the method established in this study possesses the advantages of simple operation and high-throughput, making it a promising approach for the accurate and rapid detection of DMM residues in fruit, vegetable and herbal medicine.

In some ways, the detection selectivity of an immunosensor is determined by the specificity of DMM antibody itself. Five pesticides that are structural analogues of DMM were used to validate the specificity of this fabricated IMF biosensor based on the CHA amplification strategy, including metalaxyl, metalaxyl-M, benalaxyl, flutolanil and carbendazim, and their chemical structure are shown at Fig. 5d. For the biosensor developed in this study, the fluorescence intensities of the other analogues were almost the same as that of the blank sample, and the F0/F ratio of DMM was significantly higher than those of other fungicides, as illustrated in Fig. 5c. The above results indicate that the constructed IMF biosensor exhibits high tolerance and good specificity to structurally similar fungicides.

3.5. DMM detection in real sample

DMM is classified as a high-risk pesticide in the joint health risk assessment due to its high detection rate in fruits, vegetables and herbal medicines [1,31,40], posing a potential threat to human health. In this study, the established IMF biosensor was applied to verify the practical applicability in *P. notoginseng*, *P. ginseng*, cucumber and grape, and the MRLs for DMM residue in these matrices are summarized in Table S5. The recovery experiments were conducted by spiking real samples with three different concentrations of standard DMM. As summarized in Table 2, satisfactory recoveries ranged from 86.74% to 118.60%, and low relative standard deviations (RSD, n = 3) of 2.91%–14.77% were obtained by our proposed IMF biosensor. Detailed regression analysis data are summarized in Table S6, and corresponding fluorescence spectra are shown in Fig. S2. In addition, the LC-MS/MS method was performed to further confirm the accuracy of our new biosensor assay,

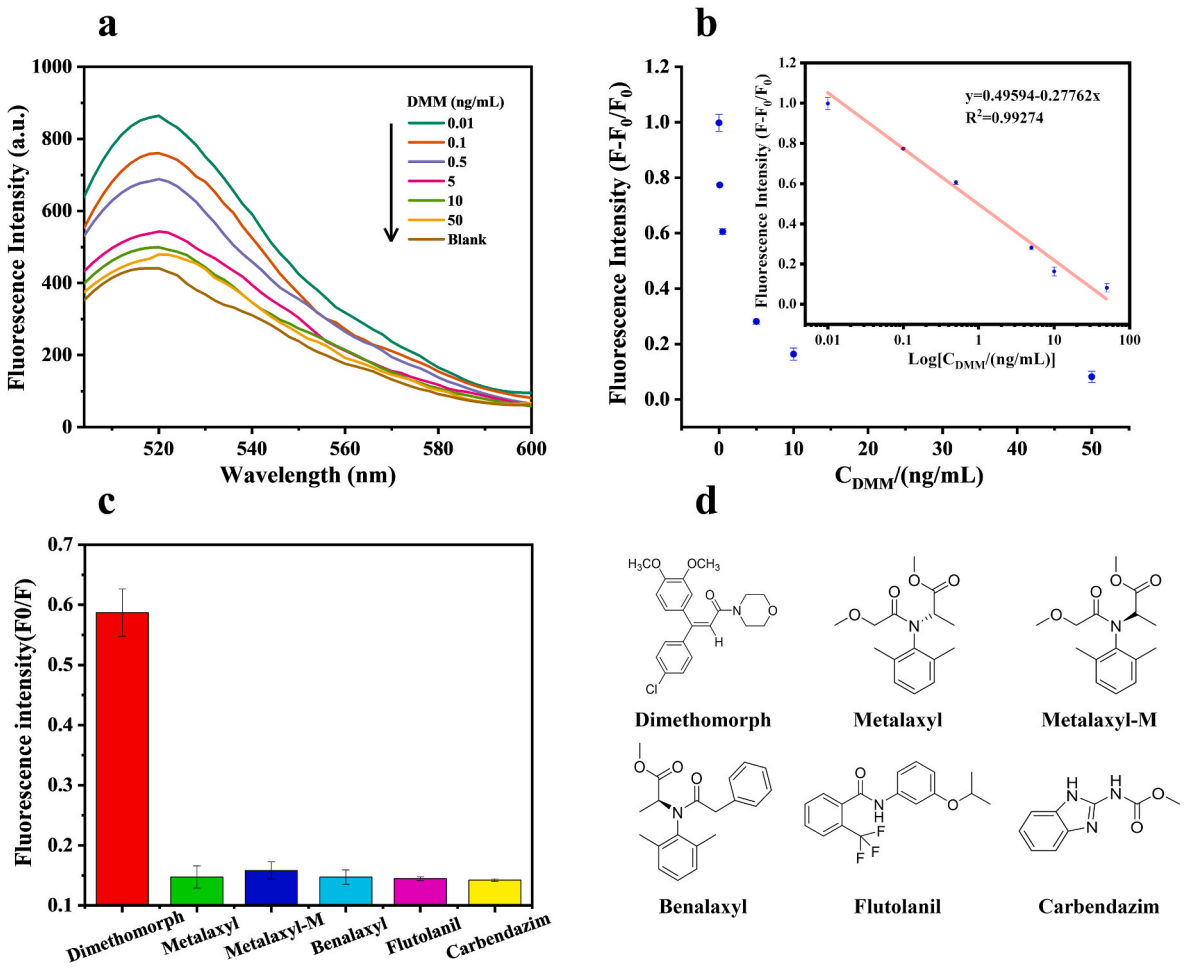

Fig. 5. The specificity and selectivity of the proposed immunofluorescence biosensor. (a) Fluorescence spectra for the detection of different concentrations of DMM; (b) linear calibration standard curve between the fluorescence intensity and logarithm of the target DMM concentration ranging from 0.01 to 50 ng/mL; (c) selectivity investigation for the analysis of DMM (10 ng/mL) compared to other fungicides including metalaxyl, metalaxyl-M, benalaxyl, flutolanil and carbendazim (10 ng/mL); (d) chemical structure of DMM and its analogue. F0/F represents the fluorescence intensity of the uncatalyzed background in blank samples relative to the catalyzed reaction in test samples. Error bars indicated the standard deviations of three experiments.

Table 1
Comparison of the sensing system for DMM detection.

Sensor type	Strategies	Samples	Linear range (ng/mL)	LOD (ng/mL)	Ref.
Electrochemical	Carbon-fibre microelectrode	water	1.22–55.85	0.15	[7]
Electrochemical	boron-doped diamond electrode	grapes and red wine	1.77–146.61	0.12	[16]
Immunochromatographic	AuNPs labeled DMM monoclonal antibody	leek	10.0–50.0	10.0	[17]
Fluorimetric	disulfide bridged β-cyclodextrin	cabbage, spinach, water and soil	0.19–7.76	0.04	[18]
Spectrophotometric	disulfide linked β-cyclodextrin	cucumber and potato	12–7500	3.70	[41]
Immunofluorescence	Au-Ab-H_0 probe and CHA amplification	grapes, cucumber, *P. ginseng* and *P. notoginseng*	0.01–50	0.002	This work

and the results obtained by the two methods were highly consistent. Therefore, our results indicate that the proposed IMF biosensor has great practical utility for the analysis of real samples.

4. Conclusions

In summary, we constructed an ultrasensitive IMF biosensor for the detection of DMM based on dual signal amplification strategy, which combines nanomaterial technology and catalytic hairpin assembly strategy. The preparation of H_0-Ab-Au probes achieved first stage signal amplification, while the introduction of a CHA cycle amplification strategy achieved second stage signal amplification. Accordingly, DMM can be quantified with ultra-high sensitivity and excellent specificity based on fluorescence signal output. Additionally, satisfactory recoveries were obtained at three concentrations from multiple complex matrices, as validated by LC-MS/MS. On the whole, our constructed IMF biosensor broadens the application of nanomaterials and CHA amplification strategies in the detection of pesticide residue. Also, it can be readily extended to other toxic and hazardous substances detection. Going forward, this biosensor has great potential to be implemented as part of a comprehensive test product or device to make it better for rapid on-site detection.

CRediT authorship contribution statement

Yunyun Wang: Writing – original draft, preparation, Data curation, Software. **Haonan Ruan:** Writing – review & editing, Data curation, Visualization. **Jing Zhang:** Data curation, Validation. **Yudan Wang:**

Table 2
Determination of DMM in real samples (n = 3).

Samples	Spiked (mg/kg)	IMF biosensor			HPLC-MS/MS		
		Detected (mg/kg)	Recovery (%)	RSD (%)	Detected (mg/kg)	Recovery (%)	RSD (%)
Panax Ginseng	0.1	0.11	110.70	14.77	0.14	103.01	1.74
	0.5	0.49	97.25	11.45	0.53	99.12	6.26
	1.0	0.87	86.74	7.66	1.03	99.07	3.94
Panax notoginseng	0.1	0.12	117.88	12.93	0.10	103.50	4.22
	0.5	0.57	114.54	7.86	0.53	106.28	4.12
	1.0	1.02	102.33	12.26	1.01	100.85	2.88
Cucumber	0.1	0.11	114.76	10.72	0.10	100.63	9.39
	0.5	0.46	92.46	5.59	0.49	98.72	4.19
	1.0	1.19	118.60	2.91	0.90	90.44	4.16
Grape	0.1	0.12	117.27	13.95	0.09	91.78	5.27
	0.5	0.59	117.01	11.41	0.50	100.42	5.78
	1.0	1.07	106.92	7.18	0.93	93.27	9.22

Validation, Software. **Mengyue Guo:** Data curation, Software. **Tongwei Ke:** Methodology, Software. **Jiaoyang Luo:** Project administration, Conceptualization, Writing – review & editing. **Meihua Yang:** Supervision, Funding acquisition, Writing – review & editing.

Declaration of competing interest

The authors declare that they have no known competing financial interests or personal relationships that could have appeared to influence the work reported in this paper.

Data availability

Data will be made available on request.

Acknowledgements

Financial support for this work was supported by the National Natural Science Foundation of China (82173971), the CAMS Innovation Fund for Medical Sciences (CIFMS, 2021-I2M-1–071, 2021-I2M-1–031), and Beijing Natural Science Foundation (7222287).

Appendix A. Supplementary data

Supplementary data to this article can be found online at https://doi.org/10.1016/j.aca.2022.340323.

References

[1] S. Lin, T. Tang, T. Cang, S. Yu, Z. Ying, S. Gu, Q. Zhang, The distributions of three fungicides in vegetables and their potential health risks in Zhejiang, China: a 3-year study (2015–2017), Environ. Pollut. 267 (2020), 115481, https://doi.org/10.1016/j.envpol.2020.115481.
[2] Y. Yang, K. Zheng, L.-P. Guo, C.-X. Wang, D.-B. Zhong, L. Shang, H.-J. Nian, X.-M. Cui, S.-J. Huang, Rapid determination and dietary intake risk assessment of 249 pesticide residues in Panax notoginseng, Ecotoxicol. Environ. Saf. 233 (2022), 113348, https://doi.org/10.1016/j.ecoenv.2022.113348.
[3] D.P. Manjarres-López, M.S. Andrades, S. Sánchez-González, M.S. Rodríguez-Cruz, M.J. Sánchez-Martín, E. Herrero-Hernández, Assessment of pesticide residues in waters and soils of a vineyard region and its temporal evolution, Environ. Pollut. 284 (2021), 117463, https://doi.org/10.1016/j.envpol.2021.117463.
[4] E. Polledri, R. Mercadante, D. Consonni, S. Fustinoni, Cumulative pesticides exposure of children and their parents living near vineyards by hair analysis, Int. J. Environ. Res. Publ. Health 18 (2021) 3723, https://doi.org/10.3390/ijerph18073723.
[5] C. Wang, Q. Zhang, F. Wang, W. Liang, Toxicological effects of dimethomorph on soil enzymatic activity and soil earthworm (Eisenia fetida), Chemosphere 169 (2017) 316–323, https://doi.org/10.1016/j.chemosphere.2016.11.090.
[6] P. Avetta, G. Marchetti, M. Minella, M. Pazzi, E. De Laurentiis, V. Maurino, C. Minero, D. Vione, Phototransformation pathways of the fungicide dimethomorph ((E,Z) 4-[3-(4-chlorophenyl)-3-(3,4-dimethoxyphenyl)-1-oxo-2-propenyl]morpholine), relevant to sunlit surface waters, Sci. Total Environ. (2014) 500–501, https://doi.org/10.1016/j.scitotenv.2014.08.067, 351–360.
[7] T.M.B.F. Oliveira, H. Becker, E. Longhinotti, D. De Souza, P. de Lima-Neto, A. N. Correia, Carbon-fibre microelectrodes coupled with square-wave voltammetry for the direct analysis of dimethomorph fungicide in natural waters, Microchem. J. 109 (2013) 84–92, https://doi.org/10.1016/j.microc.2012.03.032.
[8] J. Regueiro, N. Olguín, J. Simal-Gándara, C. Suñol, Toxicity evaluation of new agricultural fungicides in primary cultured cortical neurons, Environ. Res. 140 (2015) 37–44, https://doi.org/10.1016/j.envres.2015.03.013.
[9] J.-Y. Wang, J.-X. Li, J. Ning, X.-K. Huo, Z.-L. Yu, Y. Tian, B.-J. Zhang, Y. Wang, D. Sa, Y.-C. Li, X. Lv, X.-C. Ma, Human cytochrome P450 3A-mediated two-step oxidation metabolism of dimethomorph: implications in the mechanism-based enzyme inactivation, Sci. Total Environ. 822 (2022), 153585, https://doi.org/10.1016/j.scitotenv.2022.153585.
[10] GB 2763-2021, National Food Safety Standard–Maximum Residue Limits for Pesticides in Food, China agriculture press, Beijing, 2021.
[11] European Union, EU legislation on MRLs. https://ec.europa.eu/food/plants/pesticides/maximum-residue-levels/eu-legislation-mrls_en, 2020.
[12] Code of Federal Regulations, Title 40 - protection of environment. PART 180: tolerances and exemptions for pesticide chemical residues in food. https://www.govinfo.gov/content/pkg/CFR-2018-title40-vol26/xml/CFR-2018-title40-vol26-part180.xml, 2018.
[13] Ministry of Health, Labour and Welfare, Positive list system for agricultural chemical residues in foods. http://db.ffcr.or.jp/front/pesticide_comp, 2018.
[14] Ministry of food and drug safety, Pesticide MRLs in food. https://www.mfds.go.kr/eng/search/searchEn.do, 2017.
[15] D.G. Hayward, J.W. Wong, F. Shi, K. Zhang, N.S. Lee, A.L. DiBenedetto, M. J. Hengel, Multiresidue pesticide analysis of botanical dietary supplements using salt-out acetonitrile extraction, solid-phase extraction cleanup column, and gas chromatography–triple quadrupole mass spectrometry, Anal. Chem. 85 (2013) 4686–4693, https://doi.org/10.1021/ac400481w.
[16] F.W. de Souza Lucas, J.M. do Nascimento, V. Nogueira Freire, A.L. Melo Camelo, E. Longhinotti, P. de Lima-Neto, A. Nunes Correia, Dimethomorph electrooxidation: Analytical determination in grape-derived samples and mechanistic aspects, Electrochim. Acta 107 (2013) 350–357, https://doi.org/10.1016/j.electacta.2013.06.083.
[17] T. Xiang, X. Xu, L. Xu, L. Liu, C. Xu, H. Kuang, Gold-based immunochromatographic strip assay for detecting dimethomorph in vegetables, New J. Chem. 46 (2022) 3882–3888, https://doi.org/10.1039/D1NJ05652B.
[18] L. Yang, H. Zhao, Y. Li, Y. Zhang, H. Ye, G. Zhao, X. Ran, F. Liu, C.-P. Li, Insights into the recognition of dimethomorph by disulfide bridged β–cyclodextrin and its high selective fluorescence sensing based on indicator displacement assay, Biosens. Bioelectron. 87 (2017) 737–744, https://doi.org/10.1016/j.bios.2016.09.044.
[19] P. Yin, H.M.T. Choi, C.R. Calvert, N.A. Pierce, Programming biomolecular self-assembly pathways, Nature 451 (2008) 318–322, https://doi.org/10.1038/nature06451.
[20] J. Liu, T. Zheng, Y. Tian, Functionalized h-BN nanosheets as a theranostic platform for SERS real-time monitoring of MicroRNA and photodynamic therapy, Angew. Chem. Int. Ed. 58 (2019) 7757–7761, https://doi.org/10.1002/anie.201902776.
[21] W. Sun, Y. Wang, Z. Zhu, Y. Wang, M. Zhang, L. Jiang, S. Liu, J. Yu, J. Huang, Accurate and nonpurified identification of extracellular vesicles using dual-binding recognition mode, Anal. Chem. 93 (2021) 12383–12390, https://doi.org/10.1021/acs.analchem.1c02259.
[22] H. Chai, M. Wang, L. Tang, P. Miao, Ultrasensitive electrochemical detection of miRNA coupling tetrahedral DNA modified gold nanoparticles tags and catalyzed hairpin assembly, Anal. Chim. Acta 1165 (2021), 338543, https://doi.org/10.1016/j.aca.2021.338543.
[23] Y. Qin, D. Li, R. Yuan, Y. Xiang, Silver ion-stabilized DNA triplexes for completely enzyme-free and sensitive fluorescence detection of transcription factors *via* catalytic hairpin assembly amplification, J. Mater. Chem. B. 7 (2019) 763–767, https://doi.org/10.1039/C8TB03042A.
[24] C. Wu, S. Cansiz, L. Zhang, I.-T. Teng, L. Qiu, J. Li, Y. Liu, C. Zhou, R. Hu, T. Zhang, C. Cui, L. Cui, W. Tan, A nonenzymatic hairpin DNA cascade reaction provides high signal gain of mRNA imaging inside live cells, J. Am. Chem. Soc. 137 (2015) 4900–4903, https://doi.org/10.1021/jacs.5b00542.
[25] Y. Peng, D. Li, R. Yuan, Y. Xiang, A catalytic and dual recycling amplification ATP sensor based on target-driven allosteric structure switching of aptamer beacons, Biosens. Bioelectron. 105 (2018) 1–5, https://doi.org/10.1016/j.bios.2018.01.017.

[26] K. Saha, S.S. Agasti, C. Kim, X. Li, V.M. Rotello, Gold nanoparticles in chemical and biological sensing, Chem. Rev. 112 (2012) 2739–2779, https://doi.org/10.1021/cr2001178.
[27] G. Frens, Controlled nucleation for the regulation of the particle size in monodisperse gold suspensions, Nat. Phys. Sci. (Lond.) 241 (1973) 20–22, https://doi.org/10.1038/physci241020a0.
[28] H.D. Hill, C.A. Mirkin, The bio-barcode assay for the detection of protein and nucleic acid targets using DTT-induced ligand exchange, Nat. Protoc. 1 (2006) 324–336, https://doi.org/10.1038/nprot.2006.51.
[29] L. Zhang, Y. Mazouzi, M. Salmain, B. Liedberg, S. Boujday, Antibody-gold nanoparticle bioconjugates for biosensors: synthesis, characterization and selected applications, Biosens. Bioelectron. 165 (2020), 112370, https://doi.org/10.1016/j.bios.2020.112370.
[30] B. Li, A.D. Ellington, X. Chen, Rational, modular adaptation of enzyme-free DNA circuits to multiple detection methods, Nucleic Acids Res. 39 (2011), https://doi.org/10.1093/nar/gkr504 e110–e110.
[31] Y. Fu, X. Dou, Q. Lu, J. Qin, J. Luo, M. Yang, Comprehensive assessment for the residual characteristics and degradation kinetics of pesticides in Panax notoginseng and planting soil, Sci. Total Environ. 714 (2020), 136718, https://doi.org/10.1016/j.scitotenv.2020.136718.
[32] L. Zhang, X. Dou, C. Zhang, G. Ying, C. Liu, J. Luo, Q. Li, P. Li, Y. Wang, M. Yang, Facile preparation of stable PEG-functionalized quantum dots with glycine-enhanced photoluminescence and their application for screening of aflatoxin B1 in herbs, Sensor. Actuator. B Chem. 261 (2018) 188–195, https://doi.org/10.1016/j.snb.2018.01.124.
[33] J. Turkevich, P.C. Stevenson, J. Hillier, A study of the nucleation and growth processes in the synthesis of colloidal gold, Discuss. Faraday Soc. 11 (1951) 55, https://doi.org/10.1039/df9511100055.
[34] C.A. Mirkin, R.L. Letsinger, R.C. Mucic, J.J. Storhoff, A DNA-based method for rationally assembling nanoparticles into macroscopic materials, Nature 382 (1996) 607–609, https://doi.org/10.1038/382607a0.
[35] X. Zhang, M.R. Servos, J. Liu, Instantaneous and quantitative functionalization of gold nanoparticles with thiolated DNA using a pH-assisted and surfactant-free route, J. Am. Chem. Soc. 134 (2012) 7266–7269, https://doi.org/10.1021/ja3014055.
[36] C. Zhang, P. Du, Z. Jiang, M. Jin, G. Chen, X. Cao, X. Cui, Y. Zhang, R. Li, A.M. Abd El-Aty, J. Wang, A simple and sensitive competitive bio-barcode immunoassay for triazophos based on multi-modified gold nanoparticles and fluorescent signal amplification, Anal. Chim. Acta 999 (2018) 123–131, https://doi.org/10.1016/j.aca.2017.10.032.
[37] L.M. Demers, C.A. Mirkin, R.C. Mucic, R.A. Reynolds, R.L. Letsinger, R. Elghanian, G. Viswanadham, A fluorescence-based method for determining the surface coverage and hybridization efficiency of thiol-capped oligonucleotides bound to gold thin films and nanoparticles, Anal. Chem. 72 (2000) 5535–5541, https://doi.org/10.1021/ac0006627.
[38] C.S. Thaxton, H.D. Hill, D.G. Georganopoulou, S.I. Stoeva, C.A. Mirkin, A bio-barcode assay based upon dithiothreitol-induced oligonucleotide release, Anal. Chem. 77 (2005) 8174–8178, https://doi.org/10.1021/ac0514265.
[39] B. Su, Z. Zhang, Z. Sun, Z. Tang, X. Xie, Q. Chen, H. Cao, X. Yu, Y. Xu, X. Liu, B. D. Hammock, Fluonanobody-based nanosensor via fluorescence resonance energy transfer for ultrasensitive detection of ochratoxin A, J. Hazard Mater. 422 (2022), 126838, https://doi.org/10.1016/j.jhazmat.2021.126838.
[40] M. Celeiro, M. Llompart, J.P. Lamas, M. Lores, C. Garcia-Jares, T. Dagnac, Determination of fungicides in white grape bagasse by pressurized liquid extraction and gas chromatography tandem mass spectrometry, J. Chromatogr. A 1343 (2014) 18–25, https://doi.org/10.1016/j.chroma.2014.03.057.
[41] D. Chen, Z. Chen, K. Xu, B. Tang, Studies on the supramolecular interaction between dimethomorph and disulfide linked β-cyclodextrin dimer by spectrofluorimetry and its analytical application, J. Agric. Food Chem. 59 (2011) 4424–4428, https://doi.org/10.1021/jf200343b.